ISIJ International, Vol. 50 (2010), No. 2, pp. 302–306

Mechanical Characterization of Dual Phase Austempered Ductile Iron

Alejandro BASSO,[1] Martín CALDERA,[1] Micro CHAPETTI[2] and Jorge SIKORA[1]

1) Metallurgy Division–INTEMA, Faculty of Engineering, National University of Mar Plata, Av. Juan B. Justo 4302 (B7608FDQ) Mar del Plata–Argentina. E-mail: jsikora@fi.mdp.edu.ar 2) Welding Division–INTEMA, Faculty of Engineering, National University of Mar Del Plata, Av. Juan B. Justo 4302 (B7608FDQ) Mar del Plata–Argentina.

(*Received on August 5, 2009; accepted on October 24, 2009*)

The fatigue behavior and mechanical properties of Dual Phase Austempered Ductile Iron (Dual Phase ADI) containing 20, 50, and 70 % ausferrite were studied and compared to ductile irons with fully ferritic and ADI matrices. The results indicate that as the amount of ausferrite increases, tensile strength, yield stress, fracture toughness and fatigue resistance increase significantly, if compared to fully ferritc ductile irons. The elongation diminishes; nevertheless all Dual Phase ADI matrices have a deformation until failure that satisfies the minimum value required by ASTM A 536 standard for ferritic ductile iron. All tensile properties of the samples containing 20 % ausferrite, located in the last to freeze zones, increased; and so did the endurance limit about 25 %. The fact that Dual Phase ADI could offer a wide range of mechanical properties, as a function of the relative percentage of free ferrite and ausferrite, led to the assumption that it could be used in safety parts, thereby replacing ductile irons with other matrices.

KEY WORDS: ductile iron; dual phase ADI; microstructure; endurance limit; fracture toughness; mechanical properties.

1. Introduction

Ductile Iron (DI) production has reached a sustained growth rate over the last decades. Nowadays DI is used in the manufacture of high mechanical performance parts, replacing cast and forged steels in a large number of applications. The wide range of mechanical properties resulting from adjusting the amount and distribution of its matrix microconstituents accounts for such replacement. In fact, DI final microstructure can be properly adjusted by heat treatment; and several thermal cycles (normalizing, ferritizing, quenching & tempering, and austempering) are used in the industry to obtain different matrices (fully ferritic, ferritic-pearltic, fully pearlitic, martensitic, and ausferritic).[1–3] Nevertheless, these types of DI are not usually applied to parts in which the combination of high mechanical strength, elongation and toughness is critical. In such case, steel continues being the alternative of choice.

However, in the last years, a new type of DI, called Dual Phase ADI, has been developed to improve mechanical properties. Such an improvement has materialized in the novel microstructure this kind of DI features, composed of different amounts of allotriomorphic (or free) ferrite, and ausferrite. Hence, focus is now on obtaining high performance DI parts by using the above mentioned mixed microstructures which combine the high tensile strength and toughness of the ausferritic phase with the high elongation properties of the ferritic one.

As reported in the literature, one of the possible ways of obtaining Dual Phase ADI, is by means of a thermal cycle that involves a partial austenitization stage at temperatures within the intercritical interval of the Fe–C–Si diagram, followed by an austempering step in a salt bath.[4–7] An adequate handling of the heat treatment variables allows to control the amount, morphology and distribution of the micro constituents (free ferrite and ausferrite), thereby enabling to attain a wide range of mechanical properties.

Despite the technological interest this new kind of DI has arisen, several studies have been conducted to determine its mechanical response. The results have revealed that a strong relationship exists between tensile strength and elongation until failure in the case of some Dual Phase ADI microstructures.[4–8] Along these lines, fracture toughness tests have yielded interesting values when compared to those of fully ferritic or fully ausferritic matrices.[4] In view of the fact that many mechanical components used in the industry need tolerate cyclic loads at elevated stresses; another property to be analyzed is fatigue resistance. As yet only few authors have contributed to elucidate the fatigue behavior of this new material.

Verdu *et al.*[9] centered on the development of thermal cycles whose aim was to encapsulate graphite nodules with different amounts of ausferrite as a way to enhance mechanical and fatigue properties. These authors sought to favor the mechanical properties of ferritic DI by surrounding graphite nodules with a high resistant second phase, thus providing higher resistance to the crack initiation stage. They found that yield stress, tensile strength, and hardness increased as the ausferrite volume fraction did. In particular, microstructures composed of 80% ferrite and

20% ausferrite yielded values as high as 25% in fatigue life when compared to those of fully ferritic DI.[9)]

Considering that Dual Phase ADI parts manufacturers and users need to be aware of the quantitative values of the different mechanical properties to be used as design data, the main objective of this work is to provide a complete characterization of Dual Phase ADI containing different percentages of ferrite and ausferrite. The studies include the evaluation of fatigue behavior along with that of other mechanical properties (tensile strength, yield stress, elongation and fracture toughness). A comparative analysis among Dual Phase ADI and ductile irons with fully ferritic and fully ausferritic matrices is also included.

2. Experimental

2.1. Melts

A ductile cast iron melt was prepared using a medium frequency induction furnace at an industrial foundry plant (Megafund S.A., Argentina). The copper content chosen was 0.90% in order to optimize the material austemperability.

The melt was poured in 25 mm-thick Y-block-shaped sand moulds. Round and prismatic samples were cut from the Y-blocks and used to prepare test specimens.

2.2. Heat Treatments

All the samples employed in the present work were previously ferritized following an annealing heat treatment cycle consisting of:

(i) Austenitizing at 900°C for 3 h,
(ii) Cooling down to 740°C inside the furnace,
(iii) Holding at 740°C for 10 h,
(iv) Cooling down to room temperature inside the furnace.

The melt intercritical interval was established by employing the methodology described in previous papers by the authors.[4,5)] The lower critical temperature (Lct) was defined as 770°C, since the ferrite into austenite transformation (martensite after quenching) started at such temperature. The upper critical temperature (Uct), in turn, was fixed at 860°C, as a matrix with over 98% of martensite had been obtained from samples quenched at such temperature. Three different Dual Phase ADI microstructures, containing different relative quantities of ferrite and ausferrite, were obtained by heat treatment, consisting of a partial austenitization of the ferritic samples, by holding them into the furnace within the intercritical interval at temperatures of 800°C, 820°C, and 835°C for one hour, followed by an austempering step in a salt bath at 350°C for 90 min, in every case.

The relationship between the amount (% in volume) of ferrite and ausferrite in Dual Phase ADI microstructures was quantified by using an optical microscope and the Image Pro Plus software, following experimental procedures described in the bibliography.[10)] The reported values are the average of at least five determinations on each sample. The graphite volume was not considered in the percentage of the microconstituents informed.

Moreover samples with entirely ferritic and fully ausferritic (ADI) matrices were also used as reference materials. Standard ADI samples were obtained by means of a heat treatment comprising a complete austenitization stage at 910°C for 1 h, followed by an austempering at 350°C for 90 min.

The ferritizing and austenitization treatments were performed by using electric furnaces, while a 500 kg salt bath was used for the austempering step.

2.3. Fatigue and Tensile Tests

Fatigue tests were carried out in line with the ASTM E466-96 standard. **Figure 1** displays a scheme of the samples used. The sample dimensions were: L=20 mm, R=56 mm, D=7 mm. Four sets of samples were employed: I) Dual Phase ADI austinitized at 800°C, II) Dual Phase ADI austinitized at 835°C, III) fully ferritic DI, and IV) standard ADI.

High cycle fatigue tests were carried out using a servo-hydraulic universal testing machine ("MTS" 810) with a 661.20F.03 load cell of 10 000 kgf load capacity. All tests were performed at a stress ratio of R=0.1 (Minimum Stress/Maximum Stress) and at room temperature. Specimens were run up to failure or run-out. The number of cycles for run-out was set at 1×10^7 cycles. The sample "endurance limit" was defined as the highest stress level at which non failure occurred after 1×10^7 cycles.

Tensile tests were conducted in agreement with ASTM E8M/88 standard, using a universal testing machine (INSTRON 8501). The fracture toughness parameter K_{IC} was determined using SEN (10) standard specimens of 10×20×100 mm, following the specifications given by the ASTM E399 standard. The test specimens were pre-machined, heat treated, machined to final dimensions, notched, precracked, and tested. Notches were machined with an electro erosion machine, and precracking was conducted applying cyclic load with a double eccentric machine. The final crack length was measured using a profile projector. The values of all the properties reported are the average of testing at least three samples.

3. Results and Discussion

3.1. Material Characteristics

The chemical composition of the melt is listed in **Table 1**. The as-cast microstructure was pearlitic-ferritic, and the nodularity exceeded 90%, in agreement with the ASTM A-247 standard. The nodular count was 180 nod/mm^2. **Table 2** shows the samples identification, the austenitization tem-

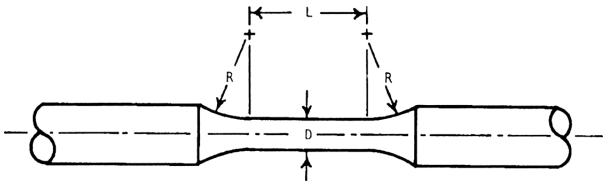

Fig. 1. Schema of fatigue test sample.

Table 1. Chemical composition (wt%).

%C	%Si	%Mn	%Cu	%Mg	%S, P	%CE
3.35	3.21	0.46	0.94	0.04	< 0.02	4.26

Table 2. Sample designation, austenitising temperature, and microconstituents percentages.

Sample	Austenitization, T (ºC)	Microconstituents in the matrix (volume %)
F	----	100% ferrite
D1	800	80% ferrite - 20% ausferrite
D2	820	50% ferrite - 50% ausferrite
D3	835	30% ferrite - 70% ausferrite
ADI	910	100% ausferrite

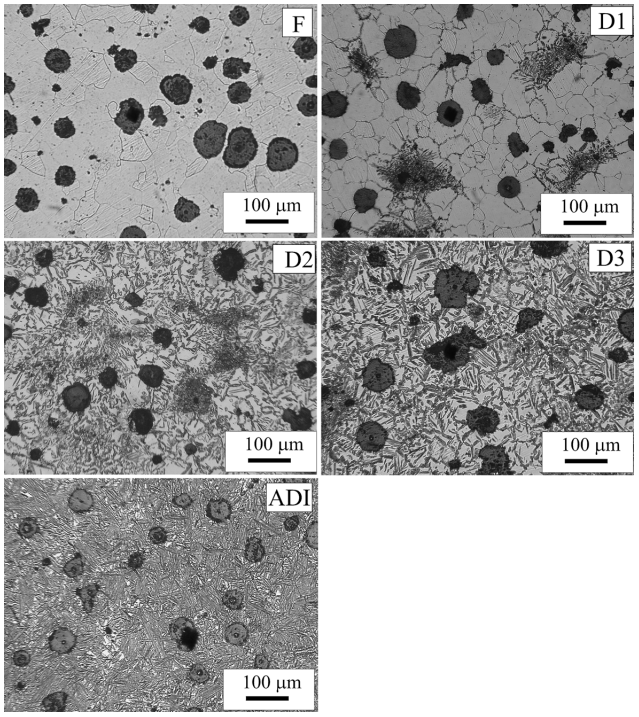

Fig. 2. Micrographs of different samples (F, D1, D2, D3, and ADI) listed in Table 2.

peratures and the final percentages of the matrix microconstituents. The relative amount of ferrite and ausferrite in Dual Phase ADI were: 80% ferrite–20% ausferrite for sample D1, 50% ferrite–50% ausferrite for sample D2, and 30% ferrite–70% for sample D3.

Figure 2 illustrates the microstructures obtained for fully ferritic DI (F), Dual Phase ADI samples austenitized at different temperatures within the intercritical interval and then austempered in the salt bath at 350°C (D1, D2 and D3), and ADI sample. As depicted in this figure, the heat treatment cycle in Dual Phase ADI allowed obtaining microstructures composed of different percentages of ausferrite and allotriomorphic ferrite (original matrix of the samples) depending on the austenitization temperature.

Retained austenite fractions were not determined because the aim of this work was to correlate the mechanical properties of Dual Phase ADI with the different amounts of allotriomorphic ferrite and ausferrite present in the microstructure. Nevertheless, it is worth mentioning that significant differences could be observed between the ausferrite present in fully ADI samples with respect to Dual Phase ADI samples.

Figure 3(a), for instance, depicts the microstructure of

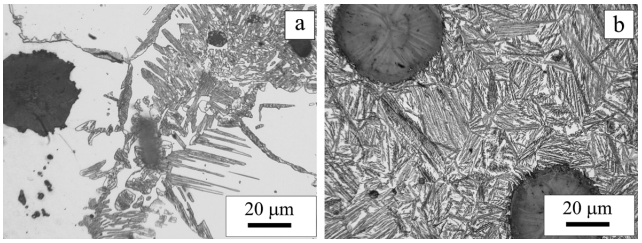

Fig. 3. Differences in morphology and distributions of ausferrite in: a) D1 sample, b) ADI sample.

sample D1 with higher magnification. In this case, the ausferrite is mainly located at the last to freeze zones (LTF), exhibiting an irregular aspect if compared with the much more homogeneous ausferrite observed in Fig. 3(b), for the entirely ausferritic ADI sample.

The differences in the characteristics of the ausferrite morphology and homogeneity are explained by the quantities of ferrite and retained austenite comprising it, which are mainly dependent on: i) differences in the chemical composition between the bulk and the LTF zones (microsegregation effect), ii) differences in the intercritical temperature between bulk and LTF (also affected by the local chemical composition), and iii) differences in the carbon content of the austenite affected by the austenitizing temperature at which each set of samples is treated.

The role that these factors play in the mechanical properties is not within the scope of this paper. Nevertheless, this subject matter could be a potential extension of future research efforts.

3.2. Fatigue Properties

Given the scarce amount of material, fatigue tests were only performed on samples with microstructures F, D1, D3, and ADI (see table 2). **Figure 4** summarizes the results of the fatigue tests for the four matrices under study. The fatigue resistance (*N*, number of cycles to failure) is plotted as a function of the applied tensile stress ($\Delta\sigma$). As noticed, fatigue resistance increases as the percentage of ausferrite present in the matrix does, and reaches its highest values in the fully ADI matrix.

This behavior can be more clearly appreciated in **Fig. 5**, in which the endurance limit is plotted as a function of the percentage of ausferrite present in the matrix. The D1 samples containing a small amount (20%) of ausferrite located in the last to freeze zones exhibit a noticeable increase if compared to fully ferritic samples (F). These results are consistent with the values accounted for by Verdu *et al.*,[9] who reported an increase in the endurance limit of around

25% for Dual Phase ADI with small percentages of ausferrite located around the graphite nodules, if compared to those in the fully ferritic DI.

Regarding D3 samples, containing 30% ferrite–70% ausferrite, the endurance limit reached a 40% increase; while a 70% increment was registered for the fully ADI matrix. Two bibliographical references were inserted in Fig. 5 for further comparison purposes. Reference 1 displays the results obtained by Venugopalan *et al.*[11] for axial fatigue properties in DI with ferritic-pearlitic matrices; whereas Reference 2 shows those obtained by Chin-Kuang Lin *et al.*[12] for ADI matrices. In both cases, the values reported are in the range of the results accounted for in this work.

3.3. Mechanical Properties

Table 3 lists the results of the tensile strength, yield stress, elongation, fracture toughness (K_{IC}), and critical crack size ($(K_{IC}/\sigma_{0.2})^2$) for samples F, D1, D2, D3 and ADI, respectively. As expected, when the amount of ausferrite increases, tensile strength, yield stress and fracture toughness do so as well, while elongation diminishes. The results of the $(K_{IC}/\sigma_{0.2})^2$ ratio revealed a maximum value for D1 samples. It is worth noticing, that, as mentioned above, the ausferritic phase is mainly located in the last to freeze zones, encapsulating the areas with the highest concentrations of small casting defects, such as inclusions, porosity, carbides, *etc.* (see Fig. 2, sample DI), as already studied by these authors.[4,5] In this case the ausferrite is thought to act as a reinforcing phase of the weakest zones, thereby increasing fracture toughness. For higher percentages of ausferrite the $(K_{IC}/\sigma_{0.2})^2$ ratio decreases given the higher values of the yield stress.

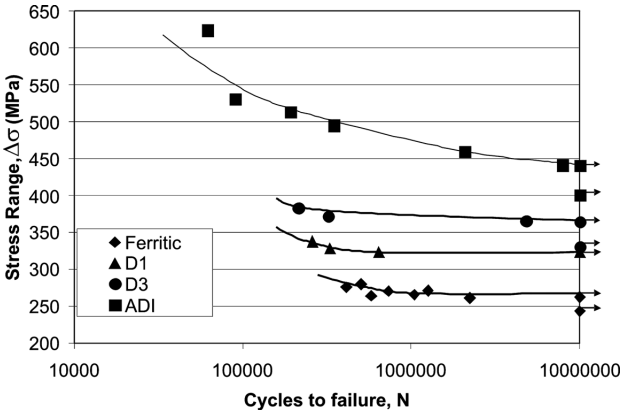

Fig. 4. σ–N curves for microstructures F, D1, D3, and ADI.

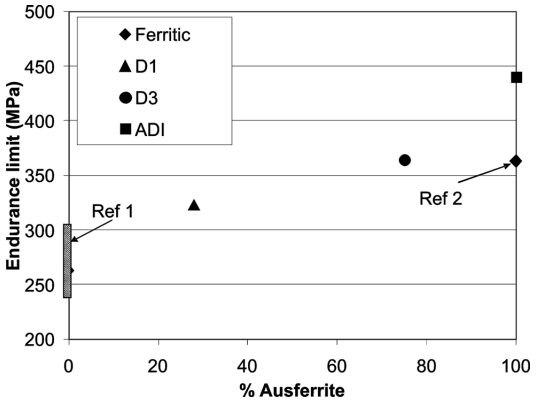

Fig. 5. Endurance limit *vs.* % of ausferrite in matrix.

3.4. Comparative Analysis among Different Matrices

Figure 6 depicts the variation (in %) of the different mechanical properties as a function of the percentage of ausferrite present in the matrix. A steady increase can be noticed in yield stress, tensile strength, endurance limit, and fracture toughness (K_{IC}) until 70% of ausferrite in the matrix with respect to a fully ferritic matrix, in which case they become more pronounced for ADI samples. This increase is attributed to the higher mechanical properties of the ausferrite in comparison with the allotriomorphic ferrite. However, it should be taken into account that other variables could affect the mechanical properties, as already mentioned in Sec. 3.1.

Nevertheless, this trend applies neither to elongation nor to critical crack size. As a matter of fact, in terms of elongation until failure, the opposite behavior was observed, yielding lower values as the amount of ausferrite increased.

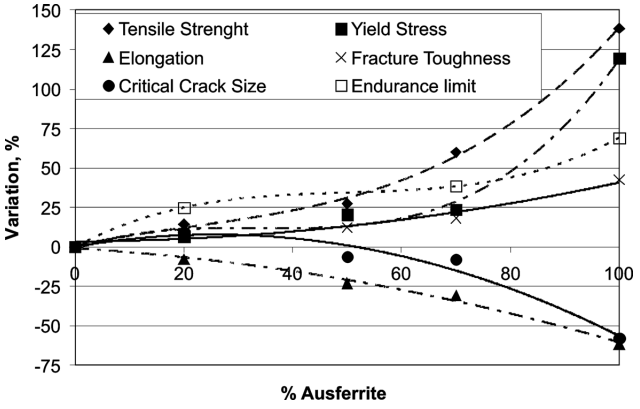

Fig. 6. Relationship between variations (%) in mechanical properties as a function of the amount of ausferrite present in the matrix.

Table 3. Mechanical properties of all matrices studied (samples D1, D2, D3, and ADI were austempered at 350°C).

Sample	σ_{max} [MPa]	$\sigma_{0.2}$[MPa]	δ[%]	K_{IC} [MPa.m$^{1/2}$]	$(K_{IC}/\sigma_{0.2})^2$ [mm]
F	455	332	26	43.6	17.2
D1	521	354	24	48.6	18.8
D2	580	400	20	49	16
D3	728	410	18	51.6	15.8
ADI	1085	729	10	62.2	7.2

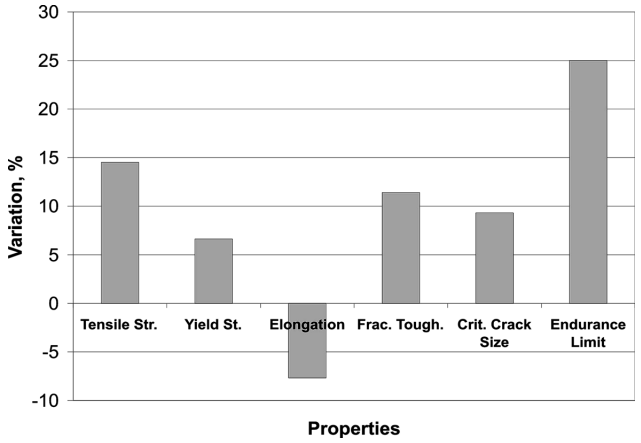

Fig. 7. Variation in tensile and fatigue properties between DI with D1 matrix and fully ferritic matrix.

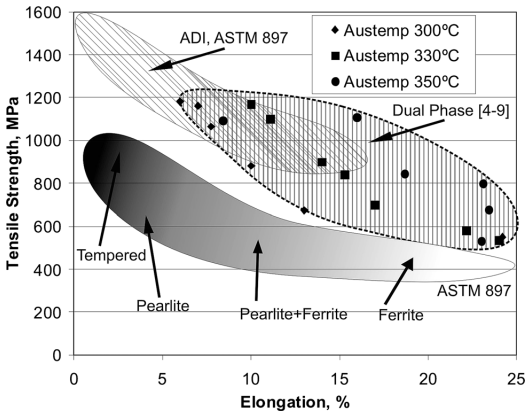

Fig. 8. Tensile strength *vs.* elongation until failure for DI with different microstructures.

As for the critical crack size, it featured a fluctuating tendency, showing its highest value in samples with 20% of ausferrite in the matrix, and the lowest in those containing 70 and 100% ausferrite.

On the basis of these results, it seems that Dual Phase ADI samples containing around 20% of ausferrite in their microstructure reveal an increase in all mechanical properties (except for elongation until failure) when compared to fully ferritic matrices. For a better interpretation of this observation, **Fig. 7** provides the increase percentages of the mechanical properties corresponding to D1 Dual Phase ADI samples in comparison with those of fully ferritic matrices. It is worth highlighting at this point that the increment in the endurance limit reaches 25%. So, the properties of this matrix variant would be improving significantly with respect to fully ferritic matrices. It is also important to point out that albeit the elongation decreases when ausferrite increases, said reduction is very small, and the deformation until failure of all Dual Phase ADI matrices keeps on meeting the minimum value required by ASTM A 536 standard (18%).

This means that Dual Phase ADI microstructures widely overcome mechanical and fatigue properties of fully ferritic matrices, preserving, at the same time, very high deformation. Indeed this combination of properties is appreciated in safety parts. Then, the fact that Dual Phase ADI could offer a wide range of mechanical properties in view of the relative microconstituents percentage present in the matrix would allow assuming that this new type of DI could replace other conventional microstructures (fully ferritic, ferritic-pearlitic, pearlitic, or tempered martensitic) since Dual Phase ADI can enhance mechanical properties combinations. This behavior is outlined in **Fig. 8**, in which the tensile strength-deformation until failure ratio is shown for DI with different microstructures, considering our results as well as those reported by other authors.[4–9)]

4. Conclusions

(1) The fatigue test revealed that an increase in the matrix ausferrite percentage increments fatigue resistance if compared to a fully ferritic matrix. A small amount of ausferrite (20%—samples D1) improves the endurance limit in around 25%.

(2) In general, when the amount of ausferrite increases, tensile strength, yield stress, and fracture toughness increase as well, while elongation diminishes. Nevertheless, such decrease is very small, and all Dual Phase ADI matrices keep having a deformation until failure that satisfies the minimum value required by ASTM A 536 standard.

(3) D1 samples yielded an increase in all the mechanical properties along with a very low decrease in the elongation until failure, in comparison with fully ferritic DI. The $(K_{IC}/\sigma_{0.2})^2$ ratio reveals the maximum value for this material variant.

(4) Dual Phase ADI could provide a wide range of mechanical properties based on the relative percentage of microconstituents present in the matrix. This would lead to the assumption that it could replace other conventional microstructures as it can favor mechanical properties combination.

Acknowledgement

The financial support granted by CONICET, SECYT and the National University of Mar del Plata is gratefully acknowledged. The help given by Eng. Nelson Alvarez Villar from CITEFA is also thankfully recognized.

REFERENCES

1) http://www.sorelmetal.com/en/ductile/frset_family.htm.
2) http://www.ductile.org/didata/Section7/7intro.htm.
3) ASM Handbook Vol. 1, Properties and Selections: Irons and Steel, Ninth edition, ASM, Ohio, USA, (1992), 33.
4) A. Basso, R. Martinez and J. Sikora: *Mater. Sci. Technol.*, **23** (2007), 1321.
5) A. Basso, R. Martinez and J. Sikora: *Mater. Sci. Technol.*, (2008) In press.
6) V. Kilicli and M. Erdogan: *Mater. Sci. Technol.*, **8** (2006), 919.
7) V. Kilicli and M. Erdogan: *Int. J. Cast Met.*, **20** (2007), 202.
8) J. Aranzabal, G. Serramoglia and D. Rousiere: *Int. J. Cast Met. Res.*, **16** (2002), 185.
9) C. Verdu, J. Adrien and A. Reynaud: *Int. J. Cast Met. Res.*, **6** (2005), 346.
10) Quantitative Microscopy, Chapter 3, Mc Graw–Hill Book Company, New York, USA, (1968), 45.
11) D. Venugopalan, K. Pilon and A. Alagarsamy: *AFS Trans.*, **96** (1988), 697.
12) C.-K. Lin and J.-Y. Wei: *Mater. Trans.*, **38** (1997), 682.